Supporting Information

Facile Synthesis of Core-Shell Structured Si/Graphene Ball as high-performance Anode for Lithium-Ion batteries

Anif Jamaluddin[1,2], Bharath Umesh[3], Fuming Chen[4], Jeng-Kuei Chang[5*], Ching-Yuan, Su[1,3,6,7*]

[1] Graduate Institute of Energy Engineering, National Central University, Taoyuan 32001, Taiwan

[2]Physic Education Department, Universitas Sebelas Maret, Jl. Ir Sutami 36 A, Surakarta, Indonesia

[3]Institute of Materials Science and Engineering, National Central University, Taoyuan 32001, Taiwan

[4] School of Physics and Telecommunication Engineering, South China Normal University, Guangzhou 510006, China

[5]Department of Materials Science and Engineering, National Chiao Tung University, Hsinchu 30010, Taiwan

[6]Depatment of Mechanical Engineering, National Central University, Taoyuan 32001,

Taiwan

[7] Research Center of New Generation Light Driven Photovoltaic Module, National Central University, Tao-Yuan 32001, Taiwan

*To whom correspondence should be addressed: (J.K. Chang) jkchang@nctu.edu.tw ; (C. Y. Su) cysu@ncu.edu.tw

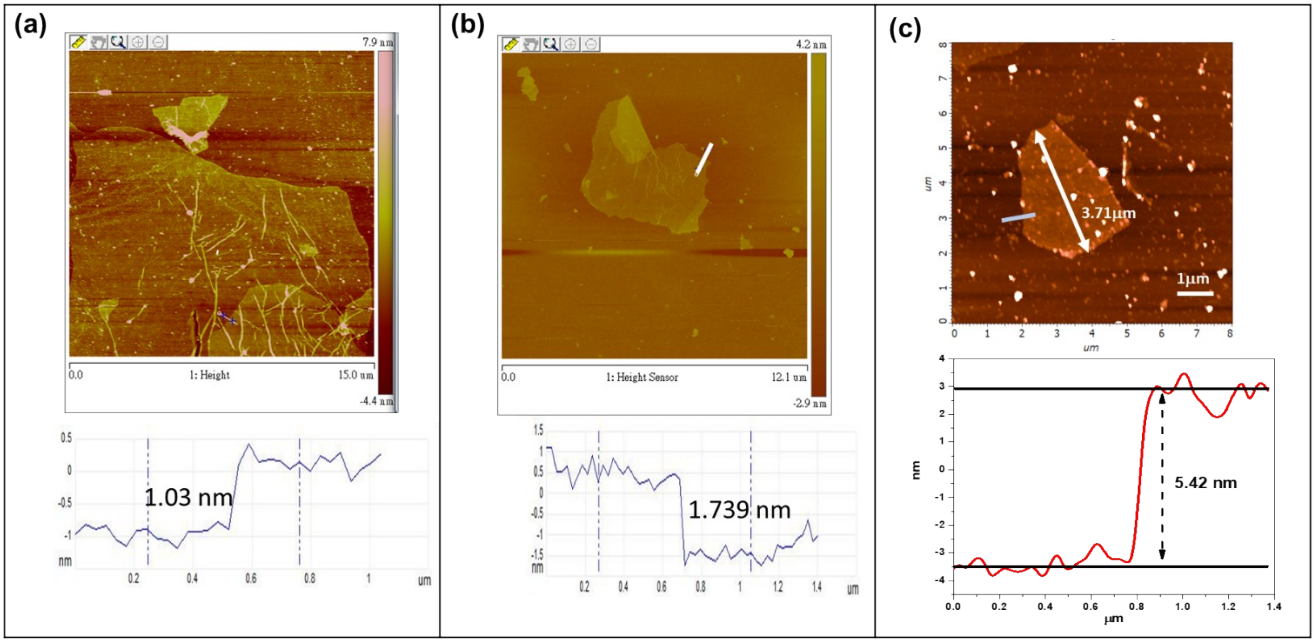

Figure S1. AFM images of: (a) graphene oxide (GO), (b) bilayer electrochemical exfoliated graphene (BL-ECG) and (c) few-layer electrochemical exfoliated graphene (FL-ECG).

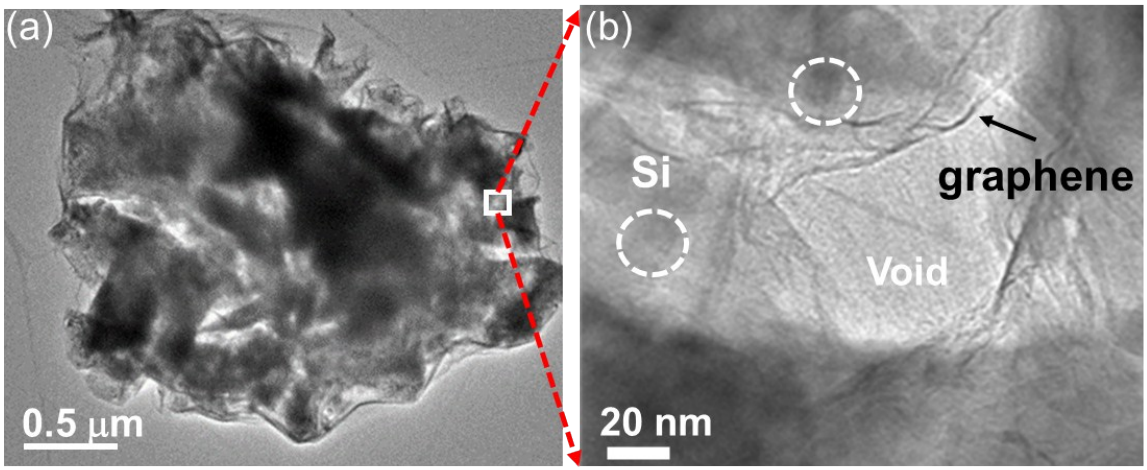

Figure S2. TEM images of the Si@BL-GB (a) microsized ball structure and a (b) high magnification image.

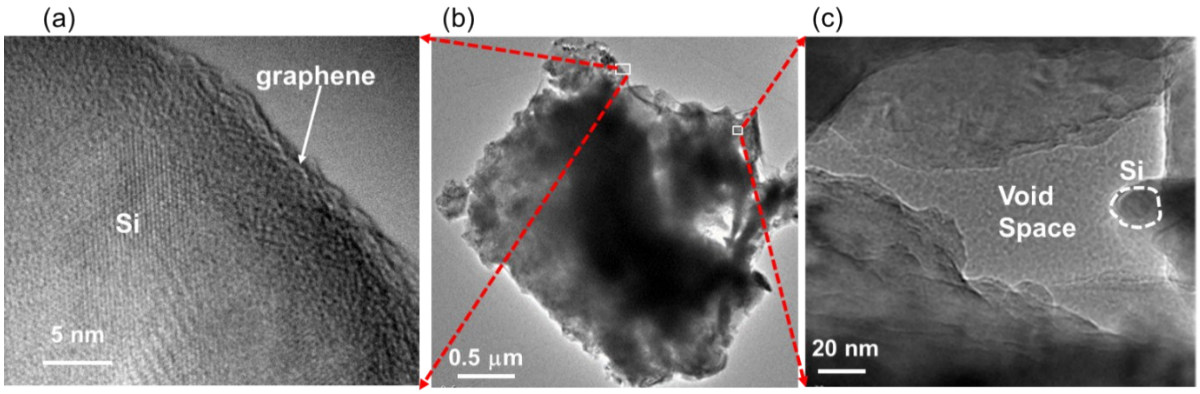

Figure S3. TEM images of Si@rGO-B: (a) high magnification of the HR-TEM image showing the graphene layer encapsulates Si NPs, (b) low magnification image of the microsized ball structure, and (c) high magnification image.

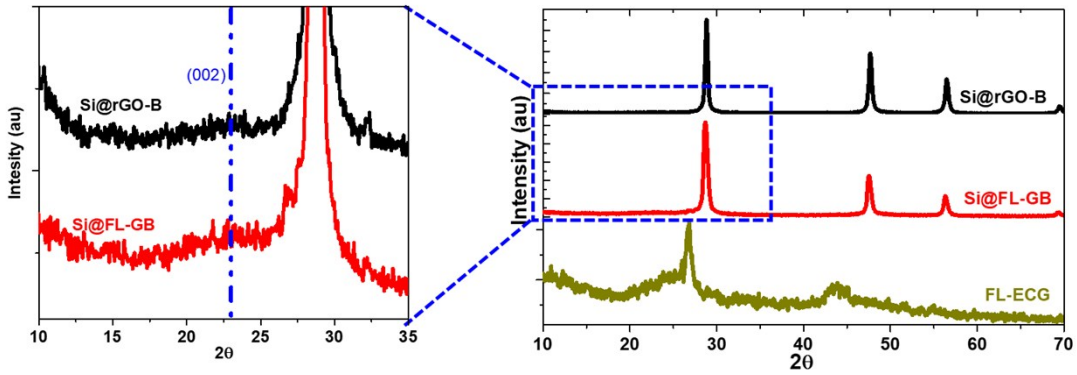

Figure S4. XRD pattern of FL-ECG, Si@FL-GB, and Si@rGO-B. The enlarged area for Si@FL-GB and Si@rGO-B, where the broadening peak at 23.34o can be identified, which is corresponding to 002 plane of graphite with interlayer spacing of ~0.34 nm.

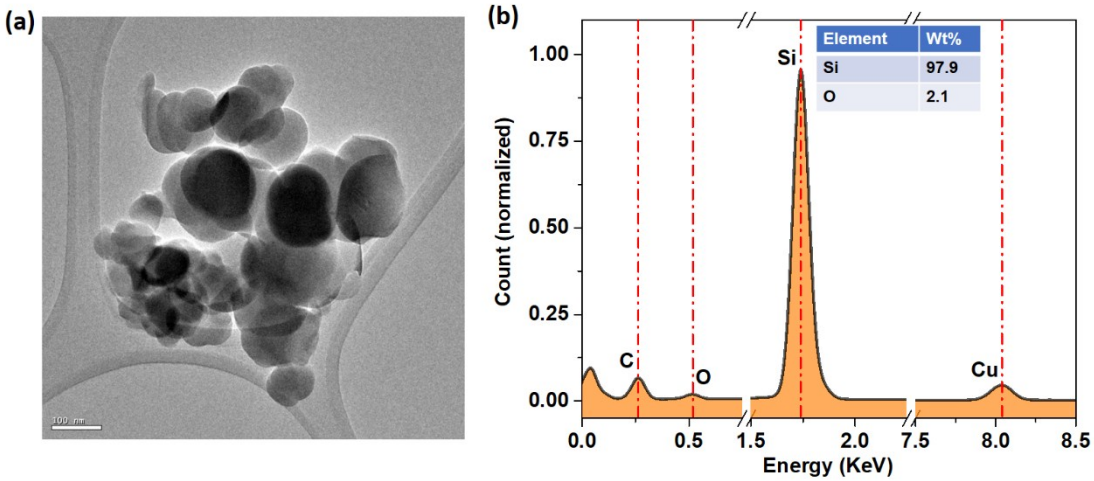

Figure S5. (a) TEM image of pure Si NPs and the corresponding EDS spectrum.

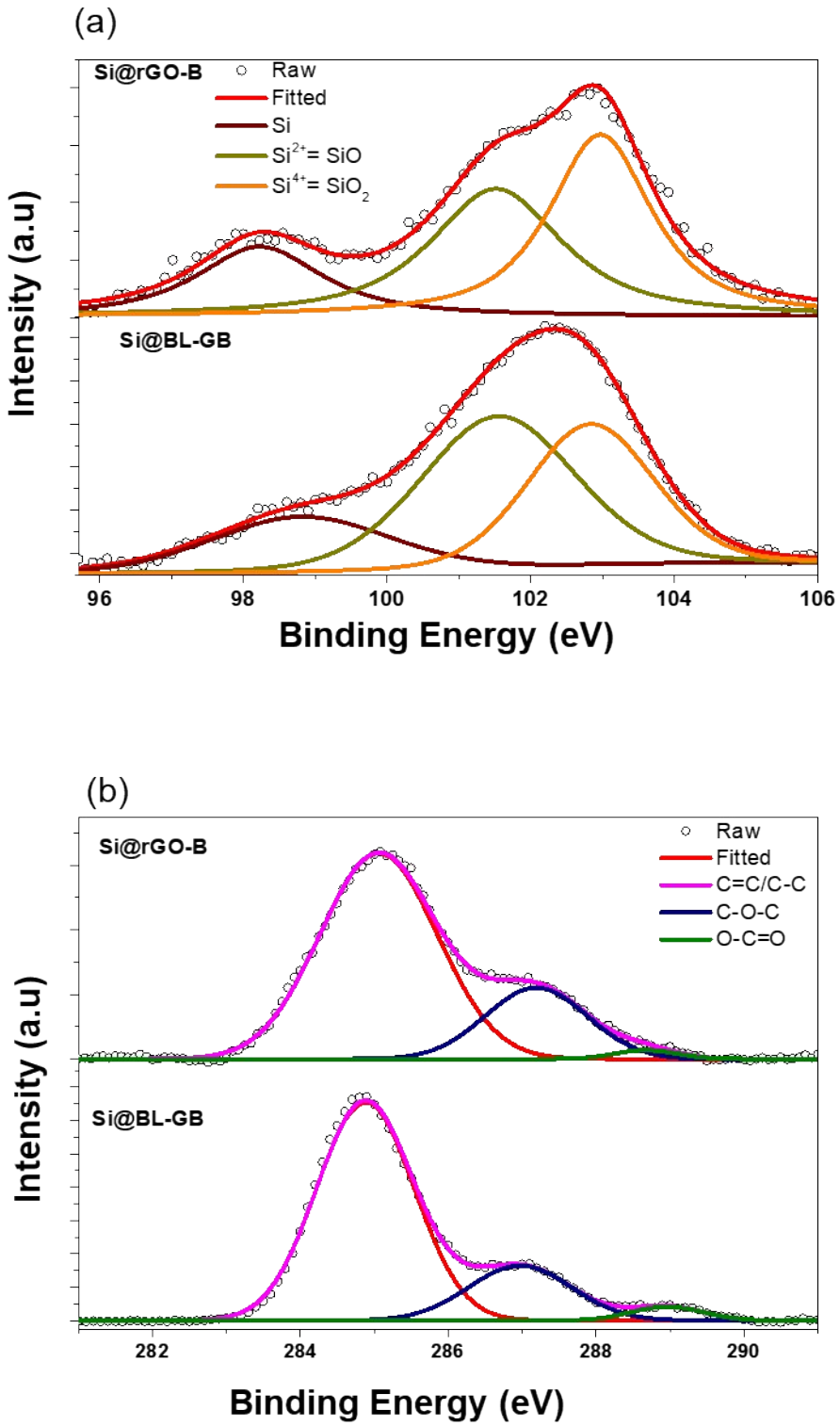

Figure S6. XPS fitting for Si@rGO-B and Si@BL-GB: (a) Si 1s spectra and (b) C 1s spectra.

Table S1. Comparison of compositional spectra of the Si@Gra composites (Si NPs, Si@rGO-B, Si@BL-GB, and Si@FL-GB) include binding energy (eV) and fraction (%).

	Si NPs	Si@rGO-B	Si@BL-GB	Si@FL-GB
Si^0	98.4 eV (23.20 %)	98.3 eV (21.51 %)	98.8 eV (19.80%)	98.2 eV (15.89%)
Si^{2+} (SiO)	101.5 eV (31.13 %)	101.2 eV (36.36 %)	101.5 eV (45.63%)	101.7 eV (28.82%)
Si^{4+} (SiO_2)	102.9 eV (45.67 %)	102.7 eV (42.13 %)	102.8 eV (34.56%)	102.9 eV (55.29%)
C=C/C-C		284.9 eV (76.11%)	284.9 (76.23%)	284.8 eV (76.91%)
C-O-C		287.4 eV (22.71%)	286.9 (20.19%)	286.6 eV (21.08%)
O-C=O		288.8eV (1.75%)	288.9 eV (3.58%)	288.66eV (2.01%)
C/O (ratio)		1.39	3.29	3.06

Table S2. The sheet resistance and C/O ratio of graphene oxide, rGO at 185 °C, BL-ECG, and FL-ECG.

Materials	Sheet Resistance ($k\Omega\ sq^{-1}$)	Thickness (μm)	C/O ratio
Graphene Oxide	~	43.13 ± 2.21	1.39
rGO (185 °C)	81.56 ±16.08	41.01 ± 1.21	2.02
BL-ECG	24.93 ± 7.58	41.11 ± 0.43	3.29
FL-ECG	5.26 ± 2.84	40.88 ± 0.56	3.79

*The sheet resistance of graphene layers is measured by 4-point probe method. The sample (graphene sheet) is coated on the glass substrate with uniform film thickness (~ 40 μm). The C/O ratio of graphene is calculated based on data from XPS instrument.

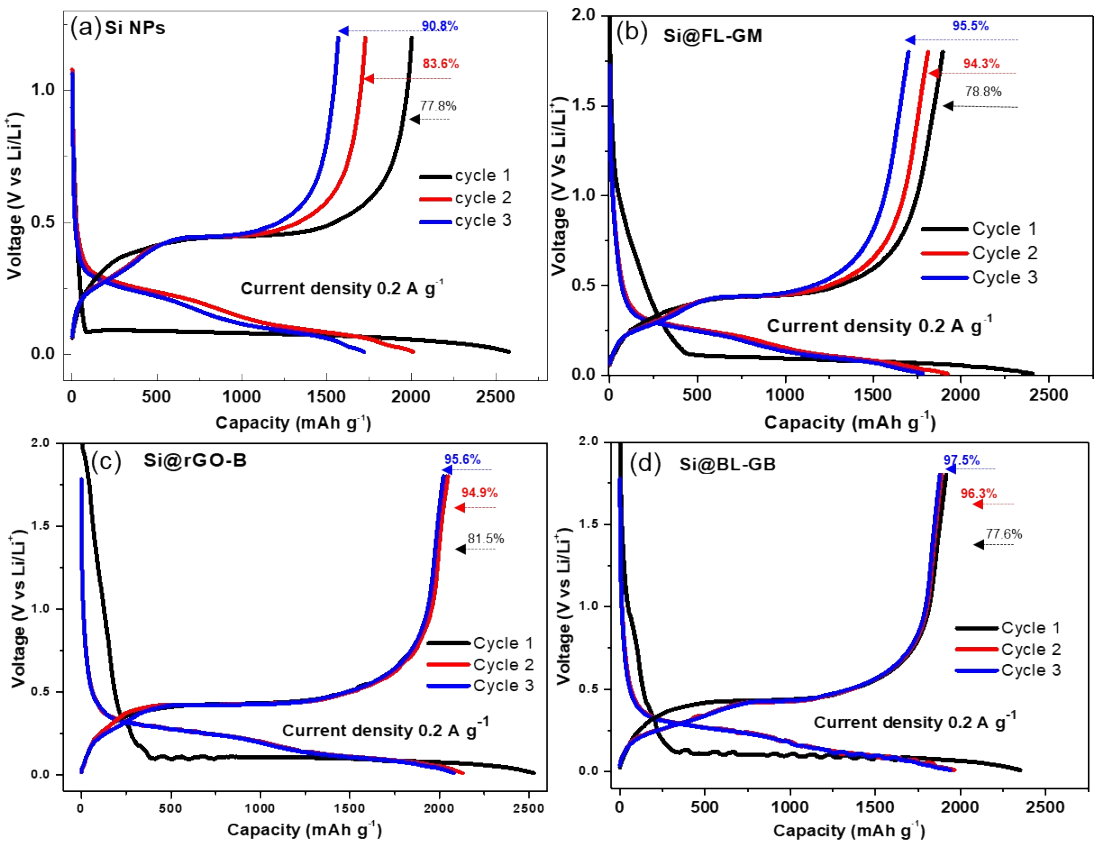

Figure. S7. The 1st, 2nd and 3rd charge-discharge performance at 0.2 A g^{-1} : (a) bare Si NPs, (b) Si@FL-GM, (c) Si@rGO-B, (d) Si@BL-GB.

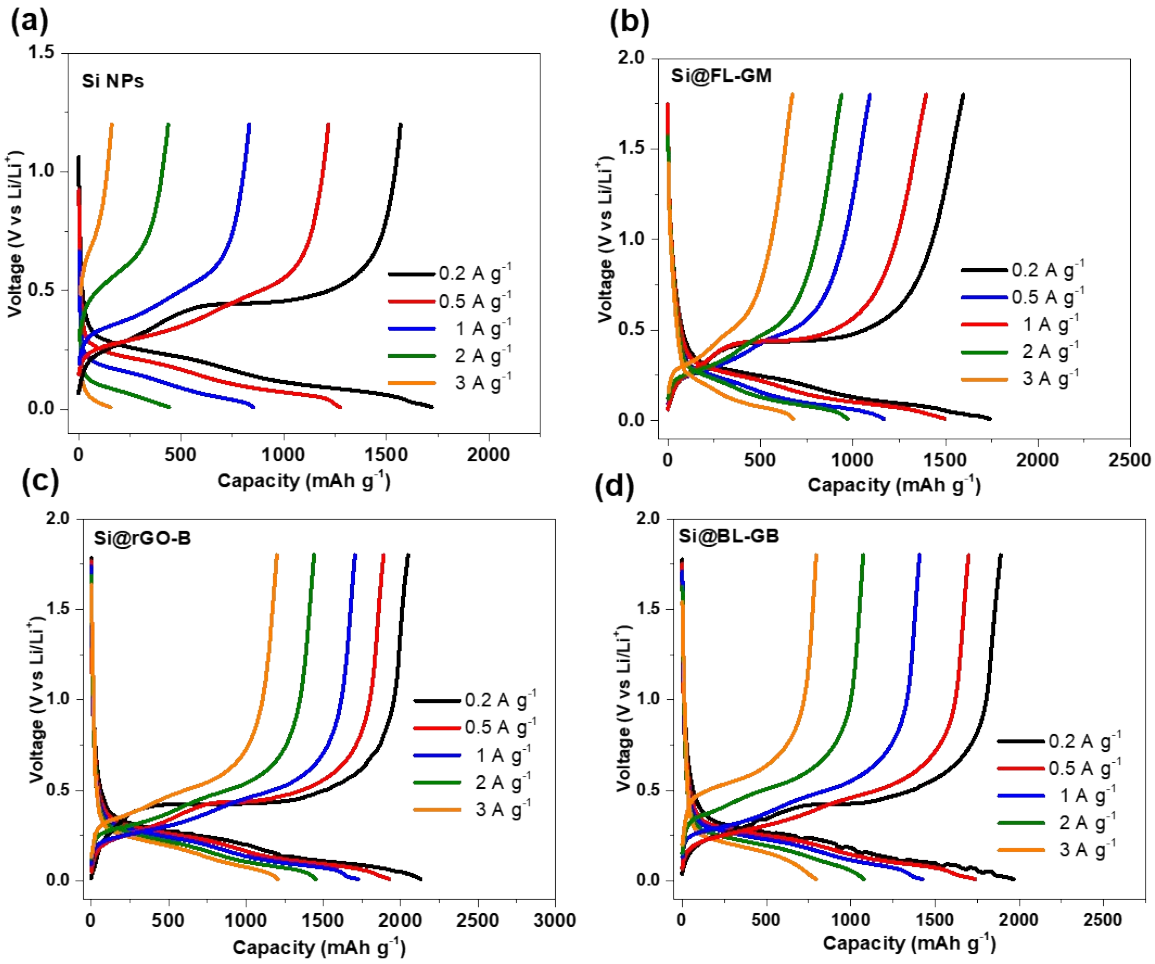

Figure. S8. The rate performance with difference current density of 0.2, 0.5, 1, 2 and 3 A g^{-1} for samples of (a) bare Si NPs, (b) Si@FL-GM, (c) Si@rGO-B, and (d) Si@BL-GB.

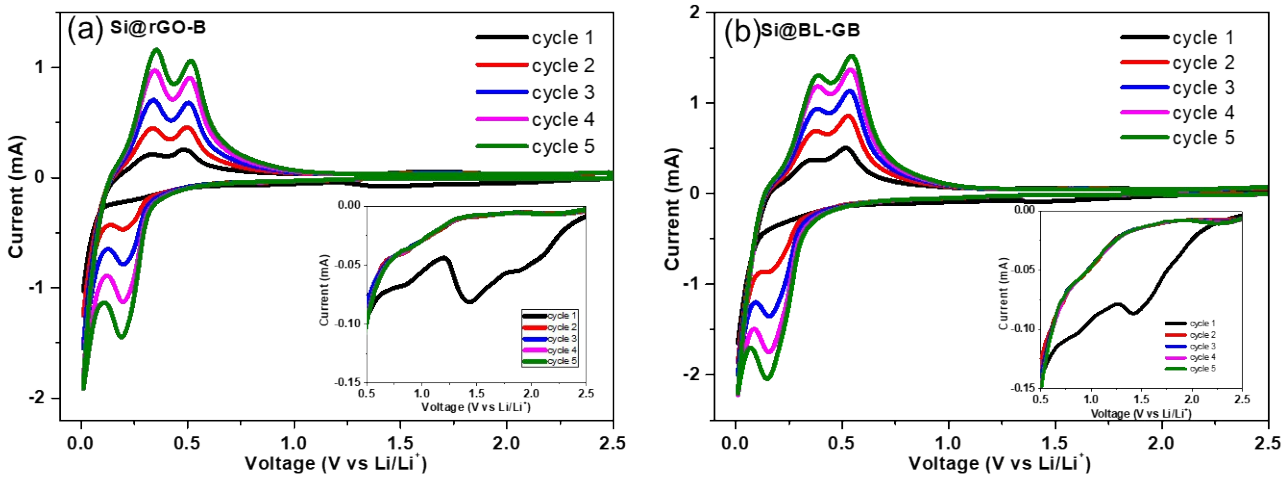

Figure. S9. CV curve with scan rate of 0.1 mV s^{-1} for (a) Si@rGO-B, and (b) Si@BL-GB. Note enlarge feature at 0.5~2.5 V.

Diffusion coefficient calculation

The lithium ion diffusion into active materials or warburg coefficient that calculated by following the equation [1, 2] :

$$Z^{'} = R_s + R_{ct} + \sigma\omega^{(-1/2)} \quad (1)$$

Where Z′ represent Warburg impedance (real part resistance), R_s= bulk resistance, R_{ct} = charge transfer resistance, $\omega = 2\pi f$ (f = frequency) angular frequency, σ= Warburg coefficient determine by the slope of the line $Z' \sim \omega^{-1/2}$.

Table S3. Resume circuit equivalent of Nyquist fitting and Warburg coefficient calculation

	Si@rGO-B	Si@BL-GB	Si@FL-GB
R_s (Ω)	16.99	17.49	17.23
R_{sei} (KΩ)	4.84	2.63	2.56
C_{sei}(mF)	2.33	2.41	0.97
C_{dl} (μF)	3.89	4.51	5.92
R_{ct} (Ω)	33.07	21.67	11.7
σ ($\Omega.s^{-1/2}$)	237.2	142.4	103.4

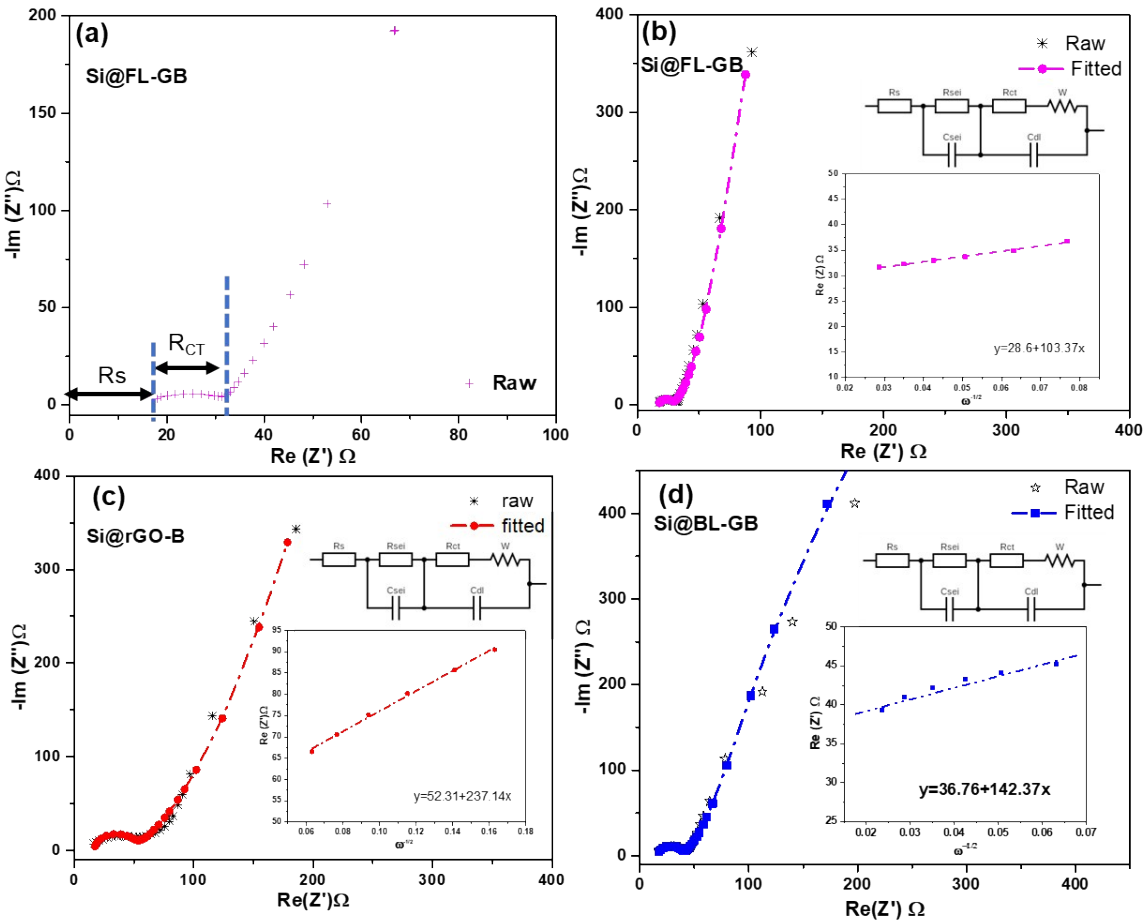

Figure S10. The Nyquist plots of (a) (b) Si@FL-GB, (c) Si@rGO-B, and (d) Si@BL-GB. Here (b) (c) and (d) show the curves fitting of the Nyquist plot and the insert curve for determining the Warburg coefficient.

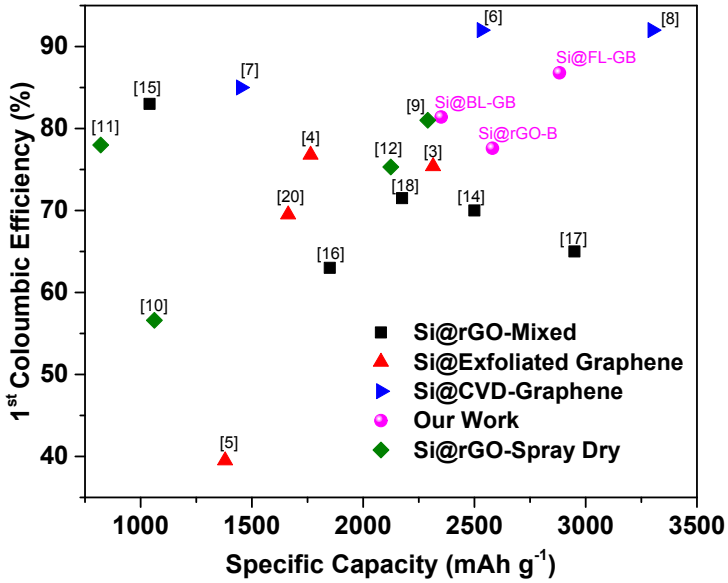

Figure S11. Comparison of specific capacity and the 1st coulombic efficiency with literature reports. Our work has excellent result, and comparable with other methods such as ball milling, simple mixing and other types of graphene include Exfoliated Graphene, Graphene Oxide, and CVD-graphene. Si@FL-GB, Si@BL-GB and Si@rGO achieve 86.9%, 81.5% and 77.6% of 1st CE, respectively. Furthermore, the comparison of rate performance and cycle stability present in Table S3.

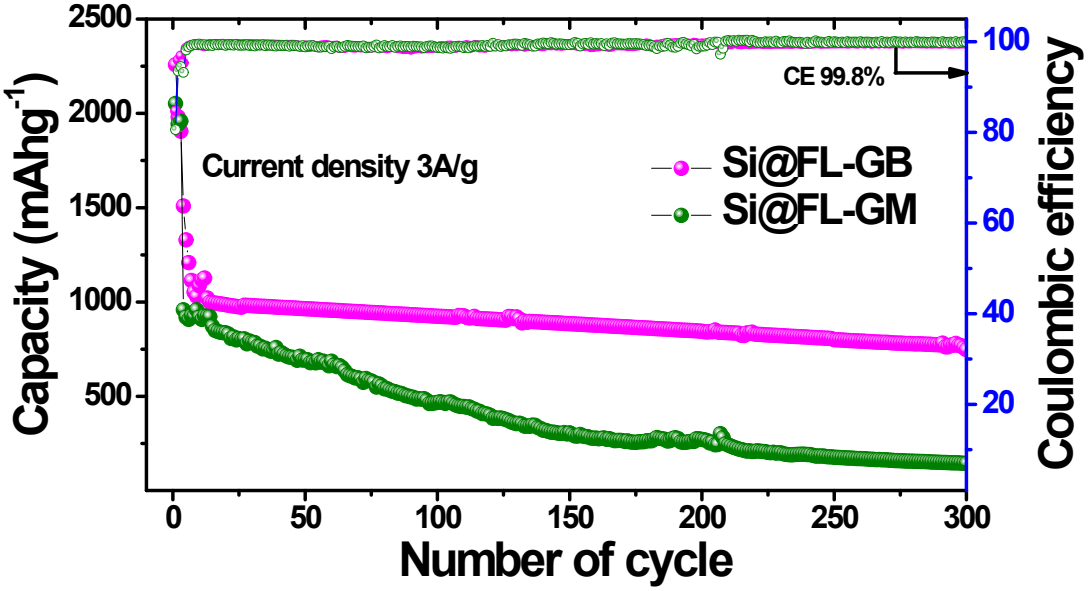

Figure S12. The stability testing at a high current density of 3A g^{-1} until 300 cycles of the Si@FL-GB and Si@FL-GM. The Si@FL-GB maintained capacity up to 747.47 mAh g-1 (99.8% of CE) with a capacity retention of 62.3% showing superior stability when compared to the Si@FL-GM, from which the capacity dropped rapidly to 144.93 mAh g^{-1} with 15.9 % of capacity retention.

Table S4. The initial capacitance, rate performance, and stability of Si@Gra composite for anode material of LIB on a different technique

No	Materials	Process	Post Treatment	1st Discharge Capacity (mAh g^{-1}), bracket current density	Performance capacity (mAh g^{-1}), bracket current density	Stability test Capacity (mAh g^{-1}), current density (A g^{-1})	References
1	Si:graphene (electrochemical exfoliation): Polydopamine	Mixing & dry	Microwave, 3-4 seconds	2314 (0.1 A g^{-1}) 75.4% (CE)	2318 (0.1 A g^{-1}) 854 (2 A g^{-1})	662 (1), 200 cycles, 98.1% (CE), 62.7% of capacity retention	[3]
2	Si:graphene	Electrolysis process	800 ^{0}C, under Ar–4% H_2	1764, 76.8% (CE)	1285 (0.2 A g^{-1}) 423 (2 A g^{-1})	2017 (0.5) A g-1, 100 cycles	[4]
3	Si: graphene (liquid phase exfoliation)	Simple mixing and drying	700 ^{0}C, 30 Min under H_2	1380, 39.5% (CE)		1500, 300 cycles, 99.8% (CE)	[5]
4	Si:graphene (CVD)	CVD with Ni template	remove template	2,532 (0.25 A g^{-1}) 92% (CE)	2500 (0.2 A g^{-1}) 500 (4.0 A g^{-1})	1385 (0.5), 95% of capacity retention	[6]
5	Si:graphene monolayer (CVD)	CVD with Cu template	remove template	1450 (0.5 A g^{-1}) 85% (CE)	3100 (0.1 A g^{-1}) 850 (3.0 A g^{-1})	1287 (0.5), 500 cycles, 89% of capacity retention	[7]
6	Si:graphene (CVD)	CVD with Ni template	remove template	3300 (4.2 A g^{-1}) 92% (CE)	2850 (0.525 A g^{-1}) 500 (16.8 A g^{-1})	1400 (2.1), 300 cycles	[8]
7	Si:PVA:Graphene Oxide (Si/C/rGO)	Spray dry	700 ^{o}C, under Ar/H_2 (9:1)	1062 (0.1 A g^{-1}) 65.6% (CE)	945 (0.1 A g^{-1}) 596 (0.5 A g^{-1})	928, 70 cycles	[9]

8	Si:Graphite:Graphene Oxide	Spray dry	450 ^{o}C, 3 h under argon	820.7 (0.05 A g^{-1}) 77.98% (CE)	820.7 (0.05 A g^{-1}) 766.2 (0.5 A g^{-1})	500 (0.1), 100 cycles	[1]
9	Si:Sucrose:Graphene Oxide	Spray dry	800 ^{o}C, 4 h under H2/Ar	2124 (0.2 A g^{-1}) 75.3% (CE)	1850 (0.1 A g^{-1}) 951 (2.0 A g^{-1})	1599 (0.1), 100 cycles, 94.9% of capacity retention	[10]
10	Si: phloroglucinol:formaldehyde	Mixing and drying	800 ^{o}C, 2.5 h under Ar	2500 (0.5A g^{-1}) 70% (CE)	1600 (0.25 A g^{-1}) 1100 (2.1 A g^{-1})	1600 (0.5) 500 cycles	[11]
11	Si:Graphene Oxide	Freeze dry	1000 ^{o}C for 1 h under Ar/H2 (95/5)	1040 (0.5 A g^{-1}) CE 83%	750 (0.05 A g^{-1}) 500 (0.25 A g^{-1})	750, 100 cycles	[12]
12	Si:GO:PAA(PolyAcrylic Acid)	Mixed and treated by Microwave radiation	700 ^{o}C under H2/Ar (95:5)	1850 (0.5 A g^{-1}) 63% (CE)	1400 (0.05 A g^{-1}) 900 (0.5 A g^{-1})	815 (0.5), 100 cycles, 80% of capacity retention	[13]
13	Si:Graphene Oxide	Modify with tetraethylorthosilicate	reacted with Mg and NaCl in 650 ^{o}C, 2 h under Ar	2949.4 (0.1 A g^{-1}) 65% (CE)	1500 (0.1 C) 1200 (5 C)	1338.1 (2.1), 100 cycles, 87.1% of capacity retention	[14]
14	Si:Graphene Oxide : PDAA (Poly (diallydimethylammonium chloride)	Mixed, dry in autoclave	450 ^{o}C for 3 h under Ar	2175 (0.1 A g^{-1}) 71.5% (CE)	1877 (0.1 A g^{-1}) 950 (5 A g^{-1})	1192, 100 cycles, 84% of capacity retention	[15]
15	Si:Graphene (Expanded Graphite)	Ball milling	NA	1663.7, 69.3% (CE)	1121(0.2 A g^{-1}) 470 (2 A g^{-1})	1055 (0.2), 50 cycles, 63.6% of capacity retention	[16]

16	Si: Few-layer graphene (Electrochemical Exfoliated graphene)	Spray Dry	NA	2882.3 (0.2 A g^{-1}) 86.9% (CE)	2567.9, (0.2 A g^{-1}) 1360.9 (3.0 A g^{-1})	1063.2 (0.5), 100 cycles, 70.9% of capacity retention	Our work
17	Si:Bi-layer graphene (Electrochemical Exfoliated graphene)	Spray Dry	NA	2351 (0.2 A g^{-1}) 81.5% (CE)	1963.9 (0.2 A g^{-1}) 794.6 (3 A g^{-1})	661.4 (0.5), 100 cycles, 57.3% of capacity retention	Our work
18	Si:Graphene Oxide	Spray Dry	NA	2581 (0.2 A g^{-1}) 77.6% (CE)	2128.4 (0.2 A g^{-1}) 1206.9 (3 A g^{-1})	787.9 (0.5), 100 cycles, 60.9% of capacity retention	Our work

Note : Coulombic Efficiency (CE)

Table S5. The BET surface area, total volume of pores, and BJH average pore diameter for the Si@FL-GB and Si@FL-GM.

	BET surface area(m^2/g)	Total volume of pores (cm^3/g)	BJH average pore diameter(nm)
Si@FL-GB	9.666	0.0481	25.34
Si@FL-GM	8.355	0.0450	31.99

References

1. M. Su, Z. Wang, H. Guo, X. Li, S. Huang, W. Xiao and L. Gan, *Electrochimica Acta*, 2014, **116**, 230-236.
2. X. Yi, W.-J. Yu, M. A. Tsiamtsouri, F. Zhang, W. He, Q. Dai, S. Hu, H. Tong, J. Zheng, B. Zhang and J. Liao, *Electrochimica Acta*, 2019, **295**, 719-725.
3. J. M. Kim, D. Ko, J. Oh, J. Lee, T. Hwang, Y. Jeon, W. Hooch Antink and Y. Piao, *Nanoscale*, 2017, **9**, 15582-15590.
4. A. R. Kamali, H.-K. Kim, K.-B. Kim, R. Vasant Kumar and D. J. Fray, *Journal of Materials Chemistry A*, 2017, **5**, 19126-19135.
5. E. Greco, G. Nava, R. Fathi, F. Fumagalli, A. E. Del Rio-Castillo, A. Ansaldo, S. Monaco, F. Bonaccorso, V. Pellegrini and F. Di Fonzo, *Journal of Materials Chemistry A*, 2017, **5**, 19306-19315.
6. C. Zhang, T.-H. Kang and J.-S. Yu, *Nano Research*, 2017, **11**, 233-245.
7. X. Ding, X. Liu, Y. Huang, X. Zhang, Q. Zhao, X. Xiang, G. Li, P. He, Z. Wen, J. Li and Y. Huang, *Nano Energy*, 2016, **27**, 647-657.
8. Y. Li, K. Yan, H.-W. Lee, Z. Lu, N. Liu and Y. Cui, *Nature Energy*, 2016, **1**.
9. H. Tao, L. Xiong, S. Zhu, L. Zhang and X. Yang, *Journal of Electroanalytical Chemistry*, 2017, **797**, 16-22.
10. Q. Pan, P. Zuo, S. Lou, T. Mu, C. Du, X. Cheng, Y. Ma, Y. Gao and G. Yin, *Journal of Alloys and Compounds*, 2017, **723**, 434-440.
11. X. Zhao, M. Li, K.-H. Chang and Y.-M. Lin, *Nano Research*, 2014, **7**, 1429-1438.
12. C. Botas, D. Carriazo, W. Zhang, T. Rojo and G. Singh, *ACS Appl Mater Interfaces*, 2016, **8**, 28800-28808.
13. F. Maroni, R. Raccichini, A. Birrozzi, G. Carbonari, R. Tossici, F. Croce, R. Marassi and F. Nobili, *Journal of Power Sources*, 2014, **269**, 873-882.
14. A. G. Kannan, S. H. Kim, H. S. Yang and D.-W. Kim, *RSC Advances*, 2016, **6**, 25159-25166.
15. B. Lee, T. Liu, S. K. Kim, H. Chang, K. Eom, L. Xie, S. Chen, H. D. Jang and S. W. Lee, *Carbon*, 2017, **119**, 438-445.
16. X. Tie, Q. Han, C. Liang, B. Li, J. Zai and X. Qian, *Frontiers in Materials*, 2018, **4**.